

Victor de Lafuente · Octavio Ruiz

The orientation dependence of the Hermann grid illusion

Received: 2 April 2003 / Accepted: 27 August 2003 / Published online: 11 November 2003
© Springer-Verlag 2003

Abstract The Hermann grid illusion (HGI), elicited by a grid displayed as either horizontal–vertical (HV) or oblique (45°) configuration, was measured as the luminance necessary to cancel the illusory spots at the grid intersections. Overall, the HGI produced by the oblique grid was about one-third of that produced by the HV grid. The observers exhibited different sensitivities to the HGI orientation, and seemed to perceive the illusion in two manners: with moderate anisotropy (reduction of about 20%, three subjects) or large anisotropy (90% reduction, four subjects). The quantitative reduction of the HGI elicited by the oblique pattern tested and its reduction to almost zero in some subjects, constitute a benchmark for any model aimed at explaining the HGI on psychophysical grounds.

Keywords Visual illusion · Center-surround receptive field · Anisotropy · Oblique effect · Inter-subject variability

Introduction

The Hermann grid illusion (HGI) is the apparent darkening of the intersections of white stripes lying on a dark background (Fig. 1a; for review see Spillmann 1994). It is currently assumed that the HGI is produced by the operation of antagonistic center-surround receptive fields (CSRFs) at the early stages of the visual pathway, with the major contribution arising from the lateral-inhibition circuits of the retina (Baumgartner 1960, as cited in Spillmann 1994). According to this view, centers of CSRFs located at the intersections of the grid would

receive more inhibition from the white stripes than those located along a stripe and flanked by two squares.

Previous works have reported a weakening of the HGI when the grid is presented obliquely (Spillmann 1971, 1994; Spillmann and Levine 1971; Levine et al. 1980) (compare Fig. 1a and b). It has been suggested that this orientation dependence involves an additional participation of higher-level mechanisms in the HGI (see page 697 in Spillmann 1994). The present article reports a quantitative assessment of the orientation dependence of one particular Hermann grid. The results are discussed in relation with lateral-inhibition CSRF models of brightness perception.

Methods

A circular patch of a Hermann grid (HG; diameter subtending 20°) was presented on a monitor, at a viewing distance of 60.5 cm. Grid parameters were chosen to produce a clearly visible HGI: stripes were of 0.7° width, and luminance 44 cd/m^2 ; squares were 2.0° in width, and 0.18 cd/m^2 luminance. The HGs looked like either Fig. 1a or b, scaled up about two-fold. The images were generated by custom software running in a computer, and displayed on a calibrated Hewlett-Packard monitor (HP70, 17-inch, 1024×768 pixels, 256 gray levels, 85 Hz). The luminance of the display area was uniform within the precision of our exposure meters (0.03 log units). The monitor was located in a light-tight cabinet to allow more precise control of its luminance.

Each observer was instructed to watch binocularly the monitor through a window furnished with a forehead rest, and to keep his or her gaze at the center of the image (indicated by a small cursor; Fig. 2a). A close-up of the subject's eyes was observed through an infrared video system. Those trials where subjects moved their eyes were discarded and repeated later. The participation of the subjects was according to the Ethical Principles of the World Medical Association.

The magnitude of the HGI was measured as the luminance of canceling disks (CDs), superimposed on the grid intersections, which made the intersections appear neither darker or brighter than the stripes (Fig. 2a) (Troscianko 1982; Schrauf et al. 1997). All the pixels composing a CD were given the same luminance, but the luminance of the CDs changed from intersection to intersection according to the formula

V. de Lafuente · O. Ruiz (✉)
Departamento de Fisiología, Biofísica y Neurociencias, Centro de Investigación y de Estudios Avanzados del IPN,
Av. IPN 2508,
07360 Mexico DF, Mexico
e-mail: oruiz@fisio.cinvestav.mx
Tel.: +55-50-613800-5107
Fax: +55-57-473754

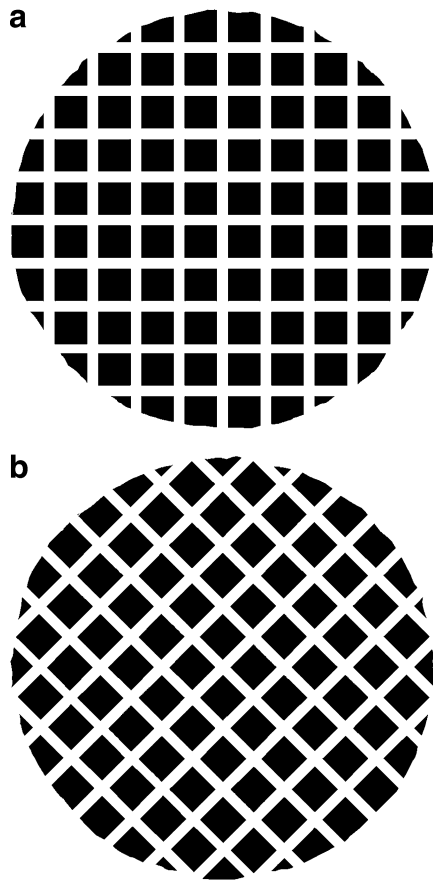


Fig. 1 a The Hermann grid illusion (HGI) is the apparent darkening of the intersections of white stripes lying on a dark background. **b** For most observers, the HGI weakens when the grid is presented obliquely

$$L(r) = \alpha r^\beta + L_0 \tag{1}$$

where $L(r)$ is the luminance of the CD (cd/m^2) located at eccentricity r (expressed as degrees of visual angle); L_0 is the luminance of the stripes (44 cd/m^2), β is an exponent controlling the shape of the CD luminance profile (see below), and α is a parameter controlling the overall luminance of the CDs (cd/m^2 per degree $^\beta$). When $\beta=0$, all the CDs on the grid exhibited the same luminance (“homogeneous luminance profile”) as determined by α . When $\beta=1$, the CD luminance became a linear function of the intersection eccentricity (Fig. 2b). In this case, α established the slope of the CD luminance profile. When $0 < \beta < 1$, or $\beta > 1$ logarithmic-like or exponential-like luminance profiles were produced, respectively.

Preliminary tests showed that observers were very sensitive to the sharp luminance border of the eight CDs located around the central intersection. The salience of these borders prevented a proper cancellation of the illusion through the grid. To overcome this problem, we smoothed the border of the eight CDs encircling the central intersection by setting the luminance of the CD borders halfway between the CD luminances and the luminance of the stripes.

Results

First experiment: the magnitude of the HGI as a function of eccentricity

The authors and two naive observers participated in a method-of-adjustment protocol to determine the overall parameters of the CDs that best canceled the HGI elicited by the tested grid. The manipulated parameters were the shape (either square or circular), size, luminance profile (β in Eq. 1), and overall luminance (α) of the canceling spots.

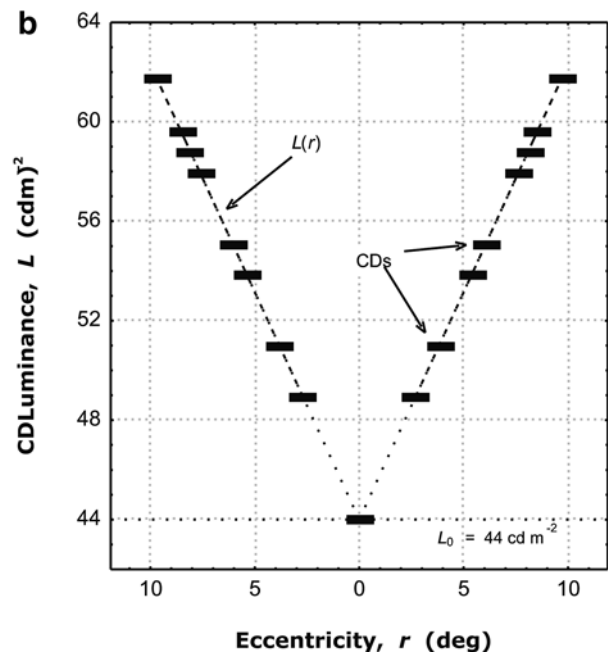
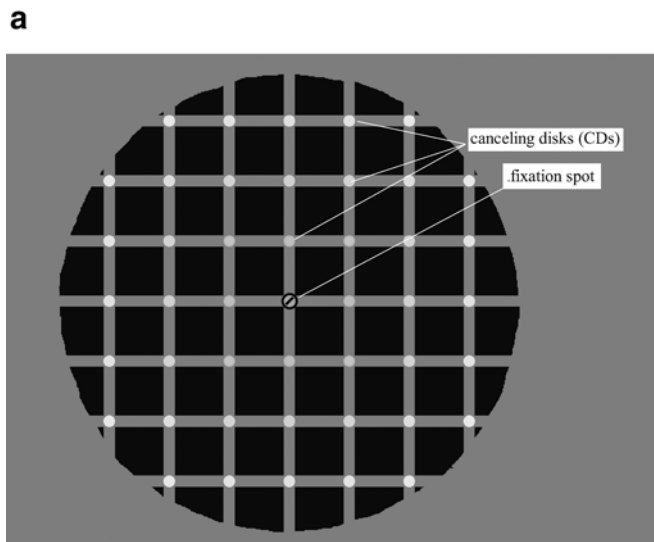


Fig. 2a,b Measurement of the Hermann grid illusion (HGI) with the cancellation technique. **a** A Hermann grid with superimposed canceling disks (CDs). **b** Luminance profile of the CDs, as a function of eccentricity. The profile shown corresponds to $\beta=1$ in

Eq. 1. The strength of the HGI was measured as the overall CD luminance (α in Eq. 1) that made the CDs appear neither darker nor brighter than the stripes

All subjects found that circular spots canceled the illusion better than squared spots. The average diameter of the CDs selected by the observers was about 1.1 times the width of the stripes. This size lies between the previously used values of 1 (Troschianko 1982) and 1.4 (Schrauf et al. 1997). All the subjects dismissed a homogeneous CD-luminance profile in favor of an increasing function of eccentricity, and chose exponent values near 1 in Eq. 1 (Fig. 2b). The shape, size and luminance profile of the CDs obtained in this experiment were used in the subsequent tests.

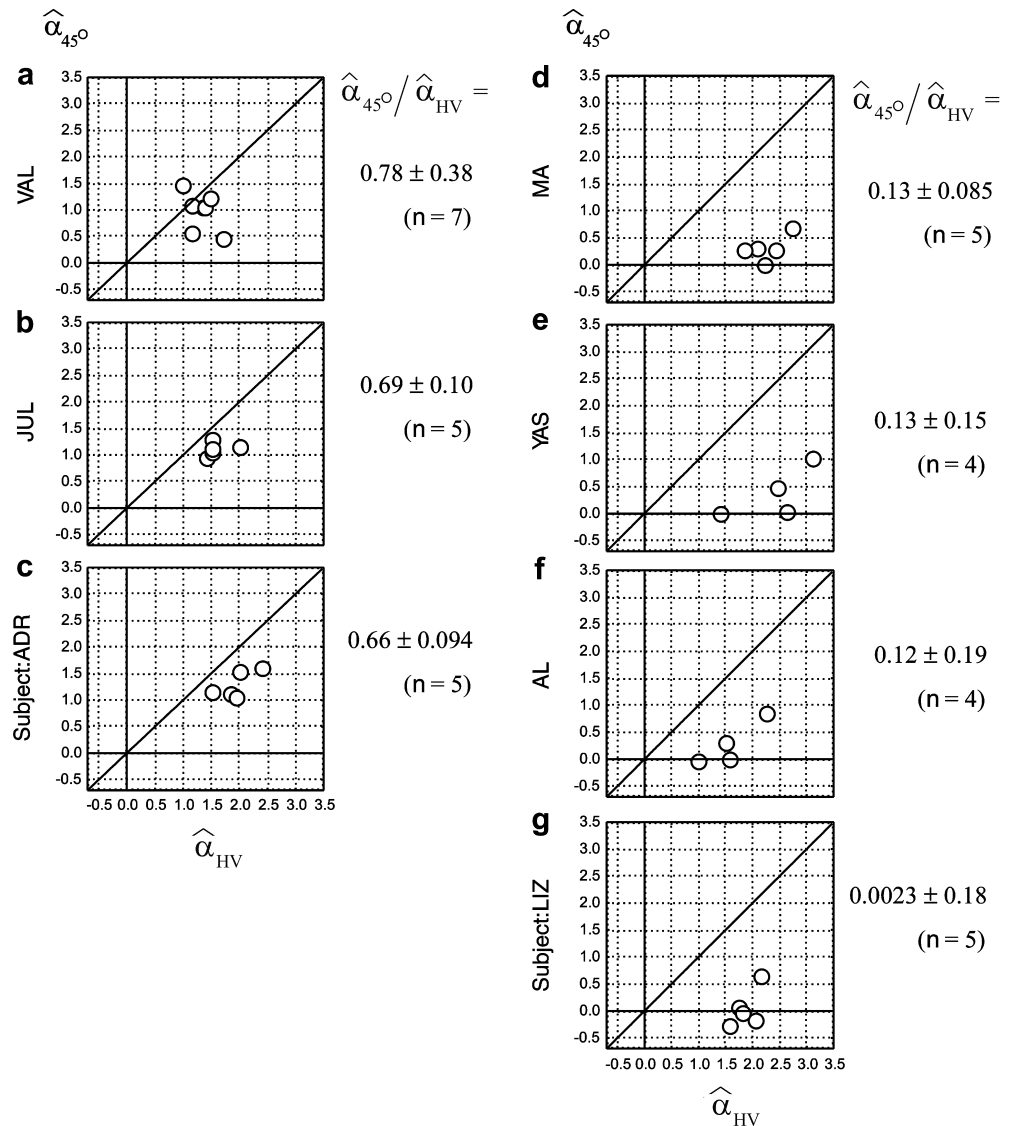
Our V-shaped CD luminance profile contrasts with the homogeneous profile used by Schrauf et al. (1997). Notice, however, that a V-shaped profile is more consistent with the non-uniform perception of the illusory spots in an HG. Except for grids made of thin stripes, the illusory spots are weakest or absent at the fixated intersection (Fig. 1).

Second experiment: orientation dependence of the Herman grid illusion

Seven subjects, between 18 and 28 years old (three males), with normal (four subjects) or corrected-to-normal vision (three subjects), unaware of the purpose of the study, participated in this experiment. Each observer completed five to eight sessions. The first session with each subject was considered as training and its results were discarded.

The magnitude of the HGI elicited by the horizontal-vertical (HV) and oblique (45°) grids was estimated by the method of constant stimuli, in a two-alternative forced-choice categorization. HGs with superimposed CDs were presented for 3 s, while the observer fixated the center of the display. When the image was substituted by a blank field, the observer reported his or her perception of the CDs through the entire pattern as “luzes” (Spanish for “lights”) or “sombras” (“dark spots”). Responses were typically made within 1–2 s after image disappearance. This protocol avoided habituation and prevented the subjects from exploring the display. Each particular

Fig. 3a–g Magnitude of the Hermann grid illusion (HGI) estimated for the horizontal-vertical (HV) and oblique (45°) grid presentations (*abscissas* and *ordinates*, respectively). Data from seven subjects (**a–g**). Each *circle* in a panel represents a measurement from one subject in one session. Most points lie below the isotropic-illusion diagonal, showing that the canceling disk (CD) luminance necessary to cancel the illusion was smaller when the grid was oblique than when it was HV. The oblique-to-HV illusion strength ratios (mean ± standard deviation) are indicated for each subject at the right of each panel



combination of grid orientation (HV or 45°) and overall CD luminance (α) was presented four times during a session, in randomized order. The responses per observer and session were used to fit psychometric functions. The α -value corresponding to the 50% probability of “lights” response, denoted as $\hat{\alpha}$, is a global measure of the illusion elicited by the whole HG. Two values of $\hat{\alpha}$ were estimated per session, one for the horizontal-vertical grid, $\hat{\alpha}_{\text{HV}}$, and one for the oblique grid, $\hat{\alpha}_{45^\circ}$.

Magnitude of the HGI

The magnitude of the HGI estimated for the HV and oblique grids is plotted in Fig. 3. Each panel corresponds to one subject. Each point within a panel denotes the estimated magnitude of the HGI elicited by the HV (abscissa) and oblique grids (ordinate), in one session. One may notice that, except for one measurement of subject VAL (Fig. 3a), all points lie below the isotropic-illusion diagonal ($\hat{\alpha}_{\text{HV}} = \hat{\alpha}_{45^\circ}$). This shows that the CD luminance necessary to cancel the HGI was smaller when the grid was oblique than when it was HV. When the data from the seven subjects were pooled together, the reduction of the HGI during the oblique-grid presentation is highly significant ($P < 10^{-6}$, Wilcoxon test).

The subjects in Fig. 3 were arranged in increasing order of HGI anisotropy. The orientation dependence of the illusion is expressed as the ratio of the oblique to HV illusion strengths per subject ($\hat{\alpha}_{45^\circ}/\hat{\alpha}_{\text{HV}}$). The values for this ratio ranged from 0.78 (weakest orientation dependence; Fig. 3a) to 0.002 (largest orientation dependence; Fig. 3g). Hence, the grid employed in this work produced a reduction of the HGI in our subjects ranging from about 20 to 100%. On average, the strength of the HGI produced by the oblique grid represented about one-third of that elicited by the HV grid: $\langle \hat{\alpha}_{45^\circ}/\hat{\alpha}_{\text{HV}} \rangle = 0.39 \pm 0.06$ (mean \pm standard error of the mean, $n=35$), median 0.32.

Variability of the estimated HGI anisotropy

The measurements of the HGI exhibits a somewhat large dispersion (Fig. 3). Kruskal-Wallis tests indicated that part of this variability is attributable to inter-subject variability ($P < 0.005$ for the HV HGI magnitude, and $P < 0.0005$ for the oblique HGI). Notice also that while the responses of some subjects tended to cluster near the isotropic diagonal (Fig. 3a–c), the responses of the others collected near the zero oblique-illusion line ($\hat{\alpha}_{45^\circ} = 0$; Fig. 3d–g). A cluster analysis of the 35 data points from the seven subjects distributed the data into two clusters, centered at $[\hat{\alpha}_{\text{HV}} \hat{\alpha}_{45^\circ}]_1 = [1.6 \ 1.1]$, and $[\hat{\alpha}_{\text{HV}} \hat{\alpha}_{45^\circ}]_2 = [2.0 \ 0.24]$, respectively ($P=0.009$ for the $\hat{\alpha}_{\text{HV}}$ coordinate, and $P < 10^{-6}$ for $\hat{\alpha}_{45^\circ}$). Except for one data point per group, this analysis neatly segregated the seven subjects in one group or the other (first group: panels a–c of Fig. 3; second group: panels d–g). Subjects belonging to the first group

would perceive an HV Hermann illusion somewhat weaker than the second group, and the illusion would be marginally (but significantly) reduced during the oblique-grid presentation, with $(\hat{\alpha}_{45^\circ}/\hat{\alpha}_{\text{HV}})_1 = 0.72$. Subjects belonging to the second group would perceive a stronger HV illusion, and a greater reduction of the illusion during the oblique-grid presentation, with $(\hat{\alpha}_{45^\circ}/\hat{\alpha}_{\text{HV}})_2 = 0.12$.

Discussion

The orientation dependence of the HGI has been reported previously (Spillmann 1971, 1994; Spillmann and Levine 1971; Levine et al. 1980). The present work confirmed those observations quantitatively by means of a novel methodology. The consequences of our results are discussed next.

The magnitude of the HGI anisotropy

This work evaluated the reduction of the HGI during the oblique presentation (45°) of a particular HG (see Methods). Further work should explore different grid parameters and orientations, and perform not only global estimations of the HGI but detailed estimations at individual intersections. Nevertheless, the reported measurements constitute, hereafter, a benchmark for any model aimed at explaining the HGI on psychophysical grounds. In particular, any HGI model should be able to predict the 20–100% reduction (average of approximately two-thirds) in the illusion strength during the oblique presentation of the grid, and its reduction to almost zero in some subjects.

Prandtl lines

The HG elicits a second type of illusion; namely, faint spurious lines running diagonally through the squares of the grid (Fig. 1b). These “Prandtl lines” are much more conspicuous in oblique grids than in HV ones (Prandtl 1927, as cited in Spillmann 1994; Goldthwaite and Crowther 1999). Pilot tests made at the beginning of this study, with HGs displayed on charts, showed that observers find it difficult to separate the effects of Prandtl lines from the HGI itself, especially in oblique grids. Moreover, some subjects noticed the Prandtl lines before the HGI. Our cancellation technique forced the subjects to react exclusively to the spots at the HG intersections. Thus, any confounding effect of Prandtl lines should have been minimized. Future work should also explore the Prandtl lines themselves and evaluate their possible relationship with the process or processes responsible for the HGI.

The HGI anisotropy and the oblique effect

Many visual tasks—but not all—are better performed when the visual patterns exhibit horizontal or vertical orientations (the “oblique effect”, OE) (Appelle 1972; McMahon and MacLeod 2003). The present work did not attempt a thorough evaluation of the OE in our subjects. However, we measured the threshold differences in an HV versus a 45° lattice detection task in five of our subjects (VAL, ADR, MA, YAS, and AL; data not shown). Contrary to the large inter-subject variability exhibited by the HGI anisotropy, the quotient of oblique to HV lattice detection contrasts did not exhibit significant inter-subject differences ($P > 0.14$, Kruskal-Wallis test), nor was it correlated with the HGI anisotropy ($P > 0.88$, Spearman rank order correlation). Hence, to the extent that this preliminary test could be representative of other OEs, we found no indication that the mechanisms responsible for the HGI anisotropy may be the same as those underlying the OE.

Inter-individual variability

We observed significant differences in the amount of HGI anisotropy exhibited by our subjects. Moreover, the distribution of measurements in our sample is consistent with a segregation of HGI anisotropies into two groups. We failed to find any obvious correlation between HGI anisotropy and visual acuity, astigmatism, sex, age, or the OE in a lattice detection task. The apparent heterogeneity of the HGI anisotropy seems to require further consideration because other orientation-dependent perceptual tasks exhibit significant inter-individual differences (Ross 1992; Fang et al. 1997; Greene et al. 2000; Liu et al. 2002). Future studies should assess whether the heterogeneity in the HGI anisotropy occurs in the general population, whether it is continuous or clustered, and whether it is correlated with any particularity in different visual tasks.

Implications of the orientation dependence of the HGI on the explanation of the illusion

Some features of the HGI are not easily explained with the standard retinal-CSRF hypothesis (e.g. Spillmann 1994). These observations are usually interpreted as indicators of additional participation of higher-level mechanisms in the illusion. In our sample, four subjects out of seven exhibited a very small HGI for oblique grids and, in three cases (YAS, AL and LIZ), the oblique illusion was indistinguishable from zero. This suggests that—at least in some subjects—the illusion would arise entirely from highly HV-biased orientation-selective mechanisms. In other words, the orientation-dependent component of the illusion would be not an additional contribution but—at least in some subjects—the major contribution to the illusion.

The origin of the anisotropic component of the HGI is yet to be determined. Attending to data from the primate visual system, two possibilities deserve consideration. First, orientation-selective cells are common in primary visual cortex (VCx) of monkeys (Ferster and Miller 2000; Ringach 2002), and monkey VCx exhibits an over-representation of horizontal and vertical orientations (Mansfield 1974; De Valois et al. 1982). In humans, while the electroretinogram displays little dependence on the orientation of flashed gratings, HV gratings produce larger responses than oblique ones, both in cortical evoked potentials (Maffei and Campbell 1970) and in functional magnetic resonance images (Furmanski and Engel, 2000). Therefore, the visual cortex seems a likely candidate for the origin of the HGI.

On the other hand, as the second consideration, retinal and lateral geniculate nucleus (LGN) cells of primates are not devoid of anisotropy and orientation biases. For instance, (i) some human ganglion cells display elongated dendritic fields, and the dendritic fields of cells located within a 13° eccentricity seem to be directed towards the fovea (Rodieck et al. 1985), (ii) in *Macaca* retina, the grating orientation preferred by most ganglion cells located between 3° and 10° eccentricity is either parallel or tangential to the line joining the cell to the area centralis (Passaglia et al. 2002), and (iii) *Macaca* LGN cells tend to prefer either radially oriented stimuli or stimuli oriented more horizontally than their polar axis (Smith et al. 1990). Hence, HV biases in retinal and LGN cells are not as clear as those in VCx and, in any case, are modest when compared with the orientation selectivity and HV bias of VCx cells (Passaglia et al. 2002; Smith et al. 1990).

The possibility that the HV selectivity and bias of retinal and LGN cells could explain the HGI anisotropy may be explored further. To such end, measurements of the HGI and other brightness effects should be contrasted with realistic simulations. The model to be used should include experimentally determined parameters about primate retinal and LGN CSRF dimensions, excitatory/inhibitory relative gains and local heterogeneities, ellipticity of the center and surround areas, and center and surround orientations as a function of the cell position in the visual field. If such a model succeeds in explaining the observed HGI anisotropy one would face, nevertheless, another problem. Thus, the same model should predict the *absence* of any reported orientation dependence in other brightness effects that are also attributed to the operation of low-level CSRFs, e.g., simultaneous brightness contrast, the “pyramid” of Vasarely, and the Craik-O’Brien-Cornsweet effect (for examples of these images see Adelson 2000).

Acknowledgements We are indebted to Dr. Ricardo Bahena for help and advise with visual acuity tests, to Dr. L. Spillmann for helpful comments at the beginning of this study, and to Dr. C. Wehrhahn and an anonymous reviewer for important comments and suggestions.

References

- Adelson EH (2000) Lightness perception and lightness illusions. In: Gazzaniga MS (ed) *The new cognitive neurosciences*. MIT Press, Cambridge MA
- Appelle S (1972) Perception and discrimination as a function of stimulus orientation: the 'oblique effect' in man and animals. *Psychol Bull* 78:266–278
- De Valois RL, Yund EW, Hepler N (1982) The orientation and direction selectivity of cells in macaque visual cortex. *Vision Res* 22:531–544
- Fang LL, Bauer J, Held R, Gwiazda J (1997) The oblique effect in Chinese infants and adults. *Optom Vis Sci* 74:816–821
- Ferster D, Miller KD (2000) Neural mechanisms of orientation selectivity in the visual cortex. *Annu Rev Neurosci* 23:441–471
- Furmanski CS, Engel SA (2000) An oblique effect in human primary visual cortex. *Nat Neurosci* 3:535–536
- Goldthwaite D, Crowther A (1999) The effect of orientation on the clarity of Hermann grid illusory lines. *Spat Vis* 12:461–465
- Greene E, Frawley W, Swimm R (2000) Individual differences in collinearity judgment as a function of angular position. *Percept Psychophys* 62:1440–1458
- Levine J, Spillmann L, Wolf E (1980) Saturation enhancement in colored Hermann grids varying only in chroma. *Vision Res* 20:307–313
- Liu B, Dijkstra TM, Oomes AH (2002) The beholder's share in the perception of orientation of 2-D shapes. *Percept Psychophys* 64:1227–1247
- Maffei L, Campbell FW (1970) Neurophysiological localization of the vertical and horizontal visual coordinates in man. *Science* 167:386–387
- Mansfield RJW (1974) Neural basis of orientation perception in primate vision. *Science* 186:1133–1135
- McMahon MJ, MacLeod DIA (2003) The origin of the oblique effect examined with pattern adaptation and masking. *J Vis* 3:230–239. DOI 10:1167/3.3.4
- Passaglia CL, Troy JB, Ruttiger L, Lee BB (2002) Orientation sensitivity of ganglion cells in primate retina. *Vision Res* 42:683–694
- Ringach DL (2002) Spatial structure and symmetry of simple-cell receptive fields in macaque primary visual cortex. *JNeurophysiol* 88:455–463
- Rodieck RW, Binmoeller KF, Dineen J (1985) Parasol and midget ganglion cells of the human retina. *J Comp Neurol* 233:115–132
- Ross HE (1992) Orientation anisotropy: some caveats in interpreting group differences and developmental changes. *Ophthalmic Physiol Opt* 12:215–219
- Schrauf M, Lingelbach B, Wist ER (1997) The scintillating grid illusion. *Vision Res* 37:1033–1038
- Smith EL III, Chino YM, Ridder WH III, Kitagawa K, Langston A (1990) Orientation bias of neurons in the lateral geniculate nucleus of macaque monkeys. *Vis Neurosci* 5:525–45
- Spillmann L (1971) Foveal perceptive fields in the human visual system measured with simultaneous contrast in grids and bars. *Pflügers Archiv* 326:281–299
- Spillmann L (1994) The Hermann grid illusion: a tool for studying human perceptive field organization. *Perception* 23:691–708
- Spillmann L, Levine J (1971) Contrast enhancement in a Hermann grid with variable figure-ground ratio. *Exp Brain Res* 13:547–559
- Troscianko T (1982) A given visual field location has a wide range of perceptive field sizes. *Vision Res* 22:1363–1369